One Large Blob and Many Streams Frosting the nearby Stellar Halo in Gaia~DR2

Koppelman, Helmer; Helmi, Amina; Veljanoski, Jovan

Published in:
Astrophysical Journal Letters

DOI:
10.3847/2041-8213/aac882

Publication date:
2018

The Astrophysical Journal Letters, 860:L11 (5pp), 2018 June 10 https://doi.org/10.3847/2041-8213/aac882

One Large Blob and Many Streams Frosting the nearby Stellar Halo in *Gaia* DR2

Helmer Koppelman, Amina Helmi, and Jovan Veljanoski
Kapteyn Astronomical Institute, University of Groningen, P.O.Box 800, 9700 AV Groningen, The Netherlands; koppelman@astro.rug.nl
Received 2018 April 30; revised 2018 May 28; accepted 2018 May 29; published 2018 June 12

Abstract

We explore the phase-space structure of nearby halo stars identified kinematically from the *Gaia* second data release (DR2). We focus on their distribution in velocity and in "integrals of motion" space, as well as on their photometric properties. Our sample of stars selected to be moving at a relative velocity of at least 210 km s^{-1}, with respect to the Local Standard of Rest, contains an important contribution from the low rotational velocity tail of the disk(s). The V_R-distribution of these stars depicts a small asymmetry similar to that seen for the faster rotating thin disk stars near the Sun. We also identify a prominent, slightly retrograde "blob" that traces the metal-poor halo main sequence reported by Gaia Collaboration et al. We also find many small clumps that are especially noticeable in the tails of the velocity distribution of the stars in our sample. Their Hertzsprung–Russell (HR) diagrams disclose narrow sequences characteristic of simple stellar populations. This stream-frosting confirms predictions from cosmological simulations, namely that substructure is most apparent among the fastest moving stars, typically reflecting more recent accretion events.

Key words: Galaxy: halo – Galaxy: kinematics and dynamics – solar neighborhood

1. Introduction

The *Gaia* second data release (DR2; Gaia Collaboration et al. 2018b) has just become available and has surpassed all expectations, as evidenced by the science verification publications accompanying its release (e.g., Gaia Collaboration et al. 2018a, 2018c, 2018d). It will take many years to fully exploit the vastness of the data set and especially the fantastic increase in accuracy. On the other hand, also because of the same reasons, already a simple first exploration of the data set yields exciting new insights.

We report here the results of the analysis of the *Gaia* DR2 set of 7 million stars with full phase-space information (derived from the astrometric and radial velocity spectrometer data; Katz et al. 2018; Lindegren et al. 2018), with the aim of identifying substructure in the nearby Galactic halo. This Galactic component is particularly important for understanding the assembly of the Milky Way in a cosmological context. It is here where we expect to find merger debris and some of the most pristine stars (Bullock & Johnston 2005; Starkenburg et al. 2017). Large photometric surveys such as the Sloan Digital Sky Survey (SDSS) and the Panoramic Survey Telescope and Rapid Response System (PanSTARRS) have uncovered large overdensities and stellar streams in the outer halo (Belokurov et al. 2006; Bernard et al. 2016), indicative of relatively recent accretion activity. However, the inner regions of the stellar halo, despite containing most of the mass, have remained more of a mystery so far, partly because of the shorter dynamical timescales. Yet it is these inner halo stars that tell us about the early assembly history of the Milky Way.

In this Letter we analyze a sample of halo stars selected from a Toomre diagram constructed from *Gaia* DR2 data (Section 2). We have inspected their kinematics and dynamics as well as their distribution in the Hertzsprung–Russell (HR) diagram (Section 3). As reported in Gaia Collaboration et al. (2018a), two clear main sequences are evident among halo stars in the Solar vicinity. Here we are able to associate at least in part the older and more metal-poor sequence to a prominent slightly retrograde "blob," hinted at in previous data sets (Carollo et al. 2007; Morrison et al. 2009; Helmi et al. 2017) but never so easily discernible. We also report the presence of several small clumps of stars that populate the tails of the kinematic distribution, including the Helmi stream (Helmi et al. 1999). Cosmological simulations of halo build-up (Helmi et al. 2003) have long predicted that substructure due to accretion should be more apparent at high velocities (see also Re Fiorentin et al. 2015, for first hints). Thus, it is very plausible that these substructures are in fact the remnants of the more recent accretion of small dwarf galaxies contributing stars to the Solar neighborhood.

2. Data and Methods

Halo stars are relatively rare (less than 1% of the stars in the Solar neighborhood; see, e.g., Helmi 2008 and references therein), hence it is paramount to have a good method of identification (see Veljanoski et al. 2018). Traditionally, halo stars have been selected on the basis of their metallicity or their large velocities with respect to the disk (see Posti et al. 2017 for a recent comparison of selection methods). Here we follow the second approach, and use the traditional Toomre diagram selection to isolate halo stars (see e.g., Bonaca et al. 2017). Although subject to biases (against halo stars that have similar motions as the disk(s)), it allows the removal of the large number of nearby disk stars that dominate the counts (Brown et al. 2005).

The Toomre diagram plots the velocity in the direction of rotation V_y against $\sqrt{V_x^2 + V_z^2}$. We use the *Gaia* DR2 sample with 6D phase-space information and consider only those stars with relative parallax error $\varpi/\sigma_\varpi > 5$, which allows us to compute distances as $d = 1/\varpi$ with relative errors of 20% at most. This sample contains 6,366,744 stars.

Figure 1 shows the Toomre diagram for the stars in this sample and located within 1 kpc from the Sun. Our reference system is oriented such that X is positive toward Galactic longitude $l = 0$, Y in the direction of rotation, and Z for Galactic latitudes $b > 0$, with the Sun located at $R_{\rm Sun} = 8.2$ kpc on the negative X-axis. The velocities are also oriented in these

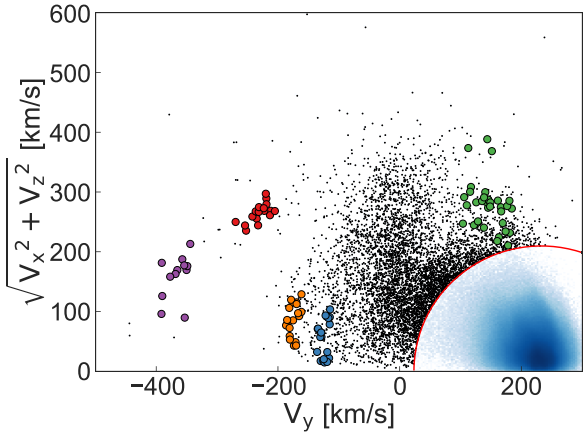

Figure 1. Toomre diagram used to identify nearby halo stars (black dots and colored circles), defined as those that satisfy $|\boldsymbol{V} - \boldsymbol{V}_{\rm LSR}| > 210$ km s^{-1}, for $V_{\rm LSR} = 232$ km s^{-1}. The density map shows the distribution of all *Gaia* DR2 stars within 1 kpc from the Sun. We consider only stars with relatively accurate parallaxes, i.e., with $\varpi/\epsilon_\varpi > 5$.

directions and have been corrected assuming a Local Standard of Rest velocity $V_{\rm LSR} = 232$ km s^{-1} (McMillan 2017) and a peculiar motion for the Sun of $(U_\odot, V_\odot, W_\odot) = (11.1, 12.24, 7.25)$ km s^{-1} (Schönrich et al. 2010).

We isolate a set of halo stars using the criterion $|\boldsymbol{V} - \boldsymbol{V}_{\rm LSR}| > V_{\rm cut}$, where we take $V_{\rm cut} = 210$ km s^{-1}, (i.e., slightly stricter than Nissen & Schuster 2010). This kinematically selected halo sample contains a total of 5980 stars, with typical velocity errors of 10 km s^{-1}. Of these, 3040 are main sequence stars. The colored solid circles in Figure 1 correspond to various easily discernable overdensities identified and discussed in more detail in the next section.

3. Analysis

3.1. Velocities

Figure 2 shows the velocity distribution of the kinematically selected halo stars. This distribution is rather complex, particularly in the $V_x - V_y$ projection (left panel of Figure 2). This is in part due to the sharpness of the selection criterion applied on the Toomre diagram. This figure also shows that slightly relaxing the value of $V_{\rm cut}$ would lead to the inclusion of more stars from the tail of the velocity distribution of the disk (s) (Schönrich & Binney 2009; Bonaca et al. 2017). Their imprint is a noticeable asymmetry in the V_x-distribution, which is characteristic of the perturbation induced by the Galactic bar (e.g., Antoja et al. 2015). In our sample, this asymmetry has a smaller amplitude than for the thin disk, but it is nonetheless clearly, and possibly unexpectedly, present at $V_y \gtrsim 100$ km s^{-1}, where the number of stars with $V_x < 0$ is 389, whereas for $V_x > 0$ there are 322 stars ($\sim 3\sigma$ excess). Properly understanding the dynamical properties of this transition region of velocity space would likely require a multi-dimensional probabilistic analysis to assign stars to different physical components using also chemical and age information (Binney et al. 2014; Posti et al. 2017), which is beyond the scope of this Letter.

The left panel of Figure 2 shows a broad overdensity of stars for positive V_x at $V_y \sim 50$ km s^{-1}, just where the contribution from the low-velocity tail of the disks would be expected to die away. Although to understand its nature requires an in-depth analysis, the location of this overdensity seems unlikely to be related to the Toomre-diagram-based selection criterion.

Figure 2 shows the presence of a prominent component with a large dispersion in V_x (equivalent to V_R near the Sun) that has a slightly retrograde mean motion of a few tens of km s^{-1}. Although this could be considered as the "traditional" halo, it is slightly too retrograde and asymmetric toward more negative V_y. Figure 2 also reveals that the high-velocity tails of the distribution of the stars in our halo sample are populated by several cold clumps. The structure at $V_y \sim 150$ km s^{-1} and $V_z \sim -250$ km s^{-1} (in green, 25 stars), can be associated with one of the streams found by Helmi et al. (1999), and also reported in Gaia Collaboration et al. (2018c) using only proper motion information (their Figure 25). The second stream found by Helmi et al. (1999) is less conspicuous with 12 stars, but present at $V_y \sim 150$ km s^{-1} and $V_z \sim 230$ km s^{-1}. The asymmetry in the number of stars in each of the streams implies that the accretion event from which these streams originate must have happened 6 to 9 Gyr ago according to the models presented in Kepley et al. (2007).

There are also other clumps in Figure 2 and these are marked with different colors. Some appear to overlap with previously reported hints of substructure (e.g., Re Fiorentin et al. 2015). For example, the orange circles are probably related to the "retrograde outlier stars" of Kepley et al. (2007), and those that are blue overlap with the structure `VelHel-4` from Helmi et al. (2017).

3.2. "Integrals of Motion"-space

Now we explore the distribution of stars in the space of "integrals of motion" defined by the z-component of the angular momentum[1] L_z, the perpendicular component $L_\perp = \sqrt{L_x^2 + L_y^2}$, and the energy E. For the stars in our sample we compute their total energy E as the sum of a kinetic and a potential term, where the amplitude of the latter is estimated using a suitable Galactic potential[2] (see Helmi et al. 2017 for details). Note that $L_\perp$ is not really conserved in an axisymmetric potential like that of our Galaxy, but nonetheless it has proven to be a useful proxy for a third integral, and helps to discriminate substructures with different orbital properties (Helmi et al. 1999; Helmi & de Zeeuw 2000).

Figure 3 shows the distribution of the halo stars in our sample in the $E - L_z$ space. Although this figure is reminiscent of that obtained using a TGAS × RAVE sample (Helmi et al. 2017) or perhaps even TGAS × SDSS (Myeong et al. 2018), it is much more spectacular.

Figure 3 shows a clear prominent "blob" or "plume" that is slightly retrograde, the counterpart of the structure seen in velocity space (Figure 2) and also in the Toomre diagram (Figure 1). This region has been previously associated with where a possible progenitor of OmegaCen would deposit debris (Dinescu 2002; Bekki & Freeman 2003; Majewski et al. 2012; Helmi et al. 2017). Whether this is the only progenitor populating this region of phase-space remains to be seen. Because of its large extent in energy, this structure contributes stars to the outer halo, and so may well be at least partly

[1] For convenience we flip the sign of the z-angular momentum such that it is positive in the sense of rotation.

[2] The exact form and values of the characteristic parameters of this Galactic potential are not too relevant, provided they yield a reasonable rotation curve for the Milky Way in the volume probed by the stars.

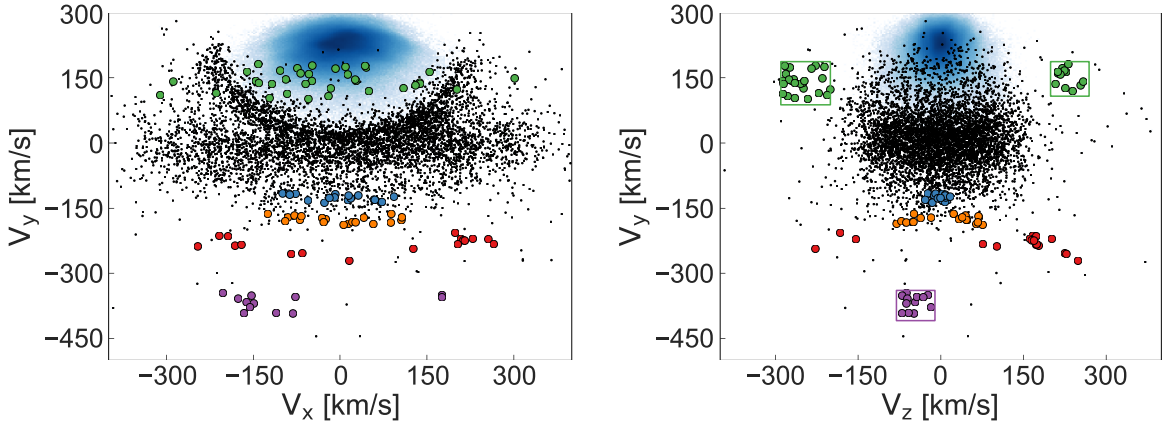

Figure 2. Velocity distribution of halo stars (black dots and colored circles) selected according to the Toomre diagram shown in Figure 1. The blue density maps show the velocity distributions of all stars within 1 kpc from the Sun and reveal the contribution of the disk(s). The left panel illustrates particularly clearly the effect of our kinematic selection criterion. The colored stars mark the location of tight clumps that are easy to discern because of their large velocities.

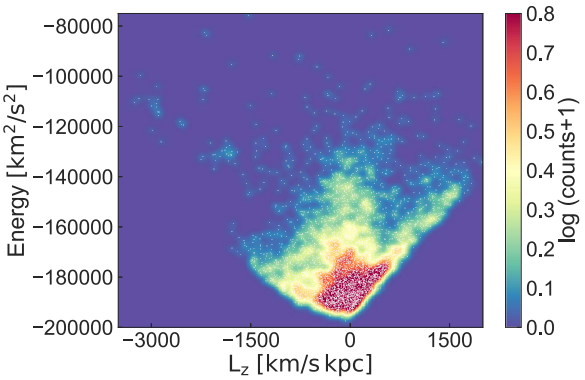

Figure 3. Distribution of the stars in our kinematically selected halo sample in the "integrals of motion" space defined by their energy E and z-component of their angular momentum L_z. To make the structure visually more apparent we have used here a stricter value of $V_{\rm cut} = V_{\rm LSR}$, which reduces the contrast between the tails of the disks and the rest of the halo.

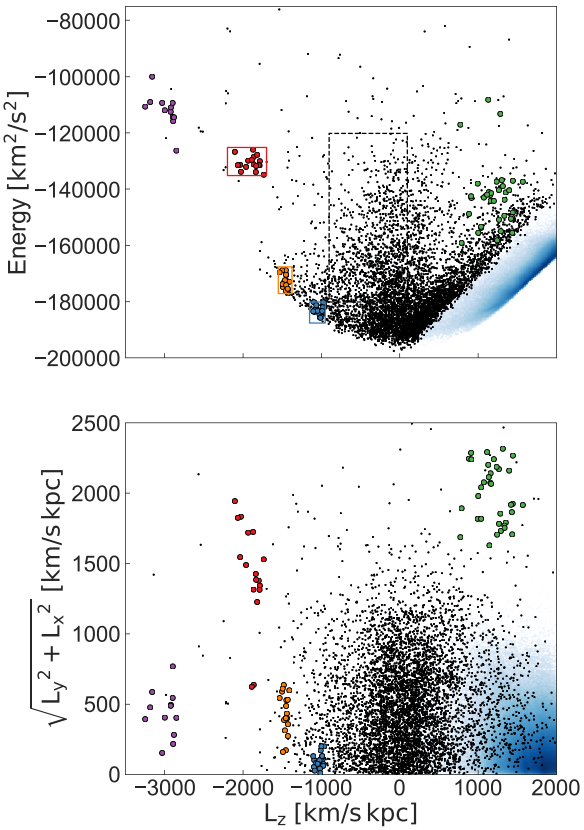

Figure 4. Distribution of stars in energy E vs. L_z (top), and in $L_\perp$ vs. L_z (bottom), highlighting the location of the various tight structures also seen in Figure 2. The blue density maps mark the contribution of all the stars in the *Gaia* DR2 6D sample located within 1 kpc from the Sun.

responsible for the "retrograde" component previously reported by Carollo et al. (2007, and subsequent work). If a single event, its size in "integrals of motion" space suggests it was very significant.

Figure 4 shows a scatter plot of the distribution of kinematically selected stars in the $E - L_z$ (top) and $L_\perp - L_z$ (bottom) spaces. We have plotted here as a density map the contribution of all the stars in the *Gaia* DR2 6D sample located within 1 kpc from the Sun and with distance errors smaller than 20%. These figures clearly show where the disks fall, as well as the sharpness of our kinematic selection criterion in the transition region between the disks and the (traditional) halo.

Several tight overdensities are also apparent in the panels of Figure 4. There is a close correspondence between these overdensities and those identified in velocity space. The boxes shown here mark the clumps that are easy to identify in the "integrals of motion" space, while the remaining colored clumps have been identified in velocity space. All of the structures have been highlighted using the same color coding as in Figure 2.

To establish the significance level of these structures we randomize the whole halo data set by reshuffling the velocities of the stars, while keeping their spatial distribution. We make 10.000 such random realizations and recompute for each the distribution in "integrals of motion" space. We find that in none of these realizations is a substructure apparent that has a similar extent and location as any of the overdensities identified in the various figures.

3.3. HR Diagram

The stars that are part of the large "blob/plume" identified in Figure 3 (inside of the gray box in the top panel of Figure 4) define a blue sequence in the HR diagram of kinematically selected halo stars, as indicated by the red dots in the large panel in Figure 5. The absolute magnitude given here is

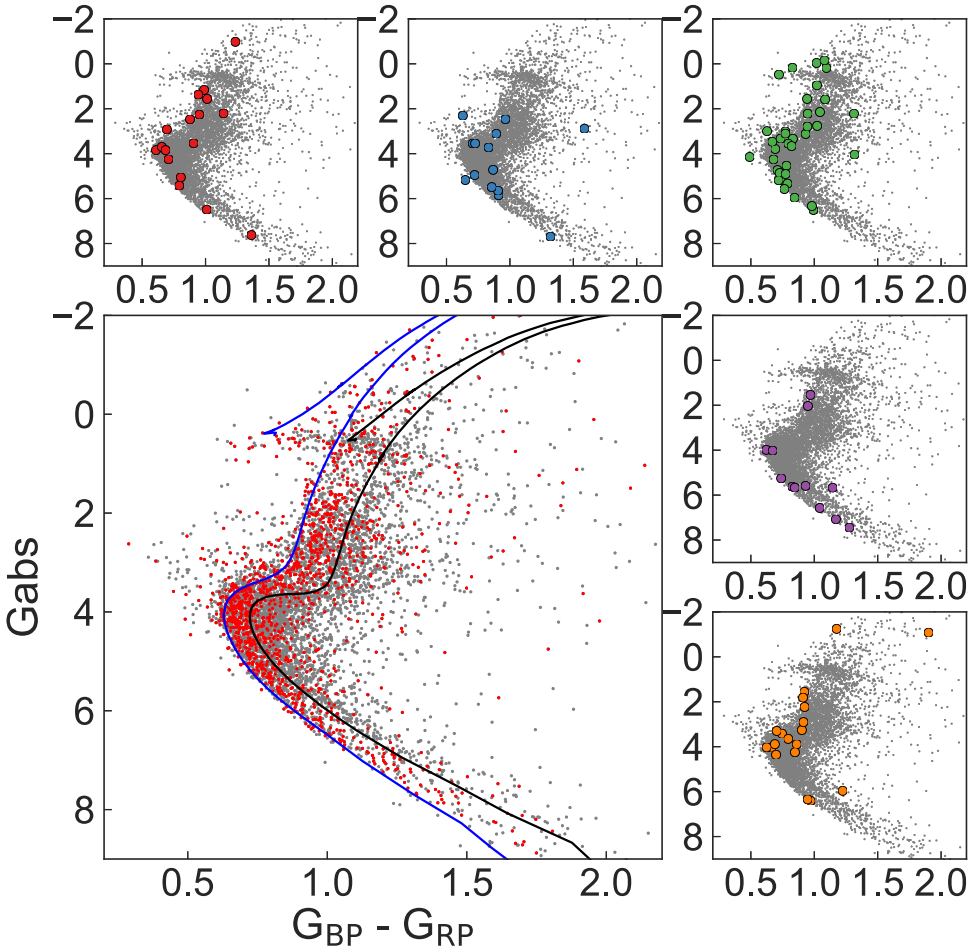

Figure 5. HR diagrams of the stars in our kinematically selected halo sample (in gray). The location of the stars in the retrograde "blob" seen in Figure 3 are shown in red in the large panel. The subpanels show the sequences defined by the other structures identified in Figures 2 and 4 using the same color schemes. To guide the eye we include here two isochrones having [M/H] ~ -1.3 dex and 13 Gyr old (blue), and [M/H] ~ -0.5 dex and 11 Gyr old (black), following Gaia Collaboration et al. (2018a).

calculated using the parallax from *Gaia* and has not been corrected for extinction. This sequence coincides with that reported by Gaia Collaboration et al. (2018a). These authors estimated an age of 13 Gyr and a metallicity [M/H] ~ -1.3 dex for this population, obtained by comparison to the blue isochrone shown here and obtained from Marigo et al. (2017), considering an α-enhancement of 0.23 (Salaris et al. 1993). The redder stars are fitted better by an isochrone with [M/H] ~ -0.5 dex and age of 11 Gyr (in black in Figure 5), as already shown in Gaia Collaboration et al. (2018a).

The stars associated with the blue sequence (and the corresponding isochrone) are more metal rich than the "outer halo" component of Carollo et al. (2007), which has [Fe/H] ~ -2.2 dex. This could imply that this region of phase-space is more complex than anticipated (see also Nissen & Schuster 2010). On the other hand, if this overdensity is due to the merger of a single large progenitor system, this could have had a metallicity gradient. This would imply that stars at larger distances could be more metal poor on average (as seen also for the streams of the Sagittarius dwarf; Bellazzini et al. 2006), thus explaining the findings of Carollo et al. (2007).

The HR diagrams for the stars belonging to the other substructures are plotted as small panels in Figure 5. We do not attempt to fit isochrones to their distribution because of the relatively low number of member stars (ranging from 12 to 37 stars). Note, however, that their HR diagrams are very coherent, and suggest low metallicities and old ages, similar to those of the large "plume" shown in the large panel of the figure. Exploration of the full *Gaia* DR2 should disclose additional members. These could be either more distant giants stars or fainter nearby dwarfs. These dwarf stars would not have full phase-space information in *Gaia* DR2 (because of the magnitude cut of the spectroscopic sample; Katz et al. 2018), but should have accurate proper motions and parallaxes, and be present in large numbers.

4. Discussion

Gaia DR2 has revealed that the phase-space structure of halo stars selected using a kinematic selection, namely in the Toomre diagram, is rather complex. It includes large overdensities and several tight kinematic streams or clumps.

The distributions of stars in velocity and in "integrals of motion" space both indicate the presence of what appears to be the low rotational velocity extension of the Galactic disks, well into the region traditionally associated to the halo. Surprisingly, this distribution is asymmetric in $V_x(V_R)$ and follows the thin disk's characteristic shape believed to be due to the effect of the Galactic bar. This is presumably the metal-rich $\sim$11 Gyr halo

component reported in the HR diagram of Gaia Collaboration et al. (2018a).

We find a prominent slightly retrograde component, which we interpret to be at least, in part, merger debris from one or more large objects. The distribution of stars in the Toomre diagram shown in Figure 1 resembles very closely Figure 7 of Villalobos & Helmi (2009), which was obtained from a simulation of the merger of a relatively massive object with a pre-existing disk (merger ratio 1:5) that subsequently gave rise to the formation of a thick disk. This large "blob" could thus have been responsible for the puffing up of an ancient Galactic disk. An alternative explanation is that this "blob" is an ancient non-rotating halo, and that the assumed Local Standard of Rest velocity should be shifted by a few tens of $\mathrm{km\,s^{-1}}$ (from the $232\ \mathrm{km\,s^{-1}}$ we assume here), which at face value seems somewhat unlikely, especially given the asymmetric shape of the "blob" toward more negative rotational velocities.

The velocity distribution of stars in our halo sample also reveals the presence of streams located in the high-velocity tails, as predicted by cosmological simulations of the build-up of galactic halos (Helmi et al. 2003). This implies that accretion has played a role in the assembly of the halo near the Sun. How important this process has been remains to be established with more sophisticated analysis. Further explorations of *Gaia* DR2 in other regions of the Galaxy, using different tracers, and only proper motion and parallax information are necessary in order to fully grasp the complexity of the stellar halo. Given the superb quality of the data, there is no doubt that *Gaia* holds many surprises for those in the quest to unravel the assembly history of the Galaxy.

We gratefully acknowledge financial support from a VICI grant to A.H. from the Netherlands Organisation for Scientific Research, NWO. This work has made use of data from the European Space Agency (ESA) mission *Gaia* (https://www.cosmos.esa.int/web/gaia), processed by the *Gaia* Data Processing and Analysis Consortium (DPAC, https://www.cosmos.esa.int/web/gaia/dpac/consortium). Funding for the DPAC has been provided by national institutions, in particular the institutions participating in the *Gaia* Multilateral Agreement. We thank Maarten Breddels for his data visualization and exploration tool: `vaex` (Breddels & Veljanoski 2018).

ORCID iDs

Amina Helmi https://orcid.org/0000-0003-3937-7641

References

Antoja, T., Monari, G., Helmi, A., et al. 2015, ApJL, 800, L32
Bekki, K., & Freeman, K. C. 2003, MNRAS, 346, L11
Bellazzini, M., Newberg, H. J., Correnti, M., Ferraro, F. R., & Monaco, L. 2006, A&A, 457, L21
Belokurov, V., Zucker, D. B., Evans, N. W., et al. 2006, ApJL, 647, L111
Bernard, E. J., Ferguson, A. M. N., Schlafly, E. F., et al. 2016, MNRAS, 463, 1759
Binney, J., Burnett, B., Kordopatis, G., et al. 2014, MNRAS, 437, 351
Bonaca, A., Conroy, C., Wetzel, A., Hopkins, P. F., & Kereš, D. 2017, ApJ, 845, 101
Breddels, M. A., & Veljanoski, J. 2018, arXiv:1801.02638
Brown, A. G. A., Velázquez, H. M., & Aguilar, L. A. 2005, MNRAS, 359, 1287
Bullock, J. S., & Johnston, K. V. 2005, ApJ, 635, 931
Carollo, D., Beers, T. C., Lee, Y. S., et al. 2007, Natur, 450, 1020
Dinescu, D. I. 2002, in ASP Conf. Ser. 265, Omega Centauri, A Unique Window into Astrophysics, ed. F. van Leeuwen, J. D. Hughes, & G. Piotto (San Francisco, CA: ASP), 365
Gaia Collaboration, Babusiaux, C., van Leeuwen, F., et al. 2018a, arXiv:1804.09378
Gaia Collaboration, Brown, A. G. A., Vallenari, A., et al. 2018b, arXiv:1804.09365
Gaia Collaboration, Helmi, A., van Leeuwen, F., et al. 2018c, arXiv:1804.09381
Gaia Collaboration, Katz, D., Antoja, T., et al. 2018d, arXiv:1804.09380
Helmi, A. 2008, A&ARv, 15, 145
Helmi, A., & de Zeeuw, P. T. 2000, MNRAS, 319, 657
Helmi, A., Veljanoski, J., Breddels, M. A., Tian, H., & Sales, L. V. 2017, A&A, 598, A58
Helmi, A., White, S. D. M., de Zeeuw, P. T., & Zhao, H. 1999, Natur, 402, 53
Helmi, A., White, S. D. M., & Springel, V. 2003, MNRAS, 339, 834
Katz, D., Sartoretti, P., Cropper, M., et al. 2018, arXiv:1804.09372
Kepley, A. A., Morrison, H. L., Helmi, A., et al. 2007, AJ, 134, 1579
Lindegren, L., Hernandez, J., Bombrun, A., et al. 2018, arXiv:1804.09366
Majewski, S. R., Nidever, D. L., Smith, V. V., et al. 2012, ApJL, 747, L37
Marigo, P., Girardi, L., Bressan, A., et al. 2017, ApJ, 835, 77
McMillan, P. J. 2017, MNRAS, 465, 76
Morrison, H. L., Helmi, A., Sun, J., et al. 2009, ApJ, 694, 130
Myeong, G. C., Evans, N. W., Belokurov, V., Sanders, J. L., & Koposov, S. E. 2018, ApJL, 856, L26
Nissen, P. E., & Schuster, W. J. 2010, A&A, 511, L10
Posti, L., Helmi, A., Veljanoski, J., & Breddels, M. 2017, arXiv:1711.04766
Re Fiorentin, P., Lattanzi, M. G., Spagna, A., & Curir, A. 2015, AJ, 150, 128
Salaris, M., Chieffi, A., & Straniero, O. 1993, ApJ, 414, 580
Schönrich, R., & Binney, J. 2009, MNRAS, 399, 1145
Schönrich, R., Binney, J., & Dehnen, W. 2010, MNRAS, 403, 1829
Starkenburg, E., Martin, N., Youakim, K., et al. 2017, MNRAS, 471, 2587
Veljanoski, J., Helmi, A., Breddels, M., & Posti, L. 2018, arXiv:1804.05245
Villalobos, Á., & Helmi, A. 2009, MNRAS, 399, 166